https://doi.org/10.46813/2023-148-101

EFFECT OF TRANSIENT LAYERS ON PLASMA ENERGY TRANSFER TO DIFFERENT SURFACES UNDER QSPA EXPOSURES

V.A. Makhlai[1,2], I.E. Garkusha[1,2], S.S. Herashchenko[1], Y.E. Volkova[1,2], Yu.V. Petrov[1], N.N. Aksenov[1], N.V. Kulik[1], D.V. Yelisyeyev[1], P.B. Shevchuk[1], T.M. Merenkova[1]
[1]National Science Center "Kharkov Institute of Physics and Technology", Kharkiv, Ukraine;
[2]V.N. Karazin Kharkiv National University, Kharkiv, Ukraine
E-mail: makhlay@kipt.kharkov.ua

The plasma energy transfer to plasma-facing materials, as well as the energy and particles exhaust, needs to be extensively studied for the implementation of the next-step fusion reactor project. Analysis of plasma-surface interaction features has been performed using QSPA exposures of reference plasma-facing materials. The parameters of the plasma streams imitated conditions of transient events in a fusion reactor. The influence of an external magnetic field on the energy balance during the plasma-surface interaction is also discussed.

PACS: 52.40.Hf; 52.70

INTRODUCTION

The lifetime of the plasma-facing components (PFCs) of the divertor, as well as the first wall, against high particle and heat fluxes during off-normal transient events (edge localized modes (ELMs), vertical displacement events (VDEs) and plasma disruptions), is still of concern in the design and realization of projects of novel fusion reactors like ITER and DEMO [1 - 3]. Erosion of PFCs caused by high-energy plasma impacts results in both surface damage and impurities production which could lead to radiative cooling of the plasma. All these aspects are critical issues for the successful performance of the fusion reactor.

One of the preliminary ITER designs proposed to use tungsten (W), CFC (Carbon Fibre Composite), and beryllium (Be) as armour materials for PFCs. Tungsten is the choice for the divertor baffle areas where a high concentration of neutral particles exists [3]. CFC was proposed for the lower part of the ITER divertor vertical targets affected by high heat fluxes. The beryllium was chosen as an armour material for ITER's first wall. Surfaces of W and Be could be damaged due to the creation and loss of a molten layer during transient events. CFCs do not melt, they have a high thermal shock and thermal fatigue resistance (low crack propagation), and high thermal conductivity [3]. However, besides brittle destruction, a general disadvantage of all carbon-based materials for fusion application is high tritium retention in redeposited layers. Therefore, CFCs were excluded from plasma-facing materials (PFM) in the last design of ITER [1, 2].

Tungsten and beryllium have low tritium retention. Additionally, W has a lower erosion rate due to its low sputtering yield and higher sputtering threshold energy compared to Be and CFC. However, tungsten has some disadvantages, including brittleness and a significant radiative power loss from the plasma even with a small amount of it present in the confined plasma region [2, 4]. Nevertheless, tungsten is proposed as a primary plasma-facing armour material for the divertor and first wall of DEMO. Consequently, comprehensive experimental investigations focusing on the selection of W grades based on their behaviour under plasma thermal loads, simulating normal heat flux, disruption, and thermal shocks are still required [1 - 6].

A liquid metal (LM) divertor was proposed as an alternative to a full metal tungsten divertor for DEMO and future fusion devices [7, 8]. LM components have a number of advantages, including the mitigation of surface melting, cracking, and embrittlement as well as the reduction of neutron-induced lattice defects that can appear in solid tungsten mock-ups [8]. It should be noted that the evaluation of plasma energy transfer to PFC produced from different materials still needs to be extensively studied experimentally.

Quasi-stationary plasma accelerators (QSPAs) have the capability to reproduce disruption and ELM impacts in terms of both heat load and particle flux to the surface which mimics the divertor conditions [9 - 12]. The energy transfer from powerful plasma to tungsten surfaces during plasma-surface interactions (PSIs) has been investigated within the quasi-stationary plasma accelerators: QSPA Kh-50 and QSPA-M [13 - 19]. The studies of vapour shielding of liquid-metal tin capillary porous structures (CPSs) under plasma loads relevant to fusion reactor transient events have been also performed in simulation experiments using QSPA experimental facilities [19]. The article presents a comparative study of the contribution of shielding layers in front of exposed surfaces to energy transfer from the powerful QSPA plasma streams to surfaces of different materials.

1. EXPERIMENTAL FACILITIES, SAMPLES AND DIAGNOSTICS

The experiments were performed within two QSPA devices: QSPA-M and QSPA Kh-50. The QSPA-M device can reproduce conditions of ITER ELM [12, 13, 18]. The discharge voltage in the QSPA-M accelerating channel achieved 10 kV and the discharge current was 400 kA. The plasma pulse duration slightly exceeded 0.1 ms. The maximum value of the hydrogen plasma pressure measured with a piezo detector amounted to 0.3 MPa. The plasma stream diameter was around 5 cm in the presence of a B-field and increased to 15 cm when the external magnetic field was switched off. The value of energy density in the axis region of the plasma stream varied in a range of 0.1 to 1 MJ/m^2 [12, 13, 18].

The average value of plasma density in free pure hydrogen plasma stream was Ne = (2...3)·10^{21} m^{-3} without an external B-field and reached Ne = (2...3)·10^{22} m^{-3} when the magnetic field was applied [12, 13].

A large-scale QSPA Kh-50 device [10, 11, 14 - 16] was used to simulate plasma disruptions and giant ELMs when a strong vapour shield dominates in plasma surface interaction significantly decreasing the energy transfer to the surface. The main parameters of the QSPA Kh-50 hydrogen plasma streams were as follows: an ion impact energy of about 0.4 keV, a maximum plasma pressure of 0.32 MPa, and a stream diameter of 18 cm. The plasma pulse shape was approximately triangular with a pulse duration of 0.25 ms. Energy density in the plasma stream achieved 3 MJ/m^2 [10, 11].

Optical spectroscopy was used for the determination of plasma parameters (electron density and temperature) in front of exposed surfaces and the studies of the target impurity behaviour in the plasma shield during the PSI [10, 13]. The plasma stream energy density and heat loads on the surface were measured with a set of movable calorimeters [11 - 16]. A high-speed (10bit CMOS pco.1200 s) digital camera PCO AG was used to perform observations of the plasma interactions with exposed targets and studies of the dynamics of material droplets and solid dust particles in front of the irradiated surface. The velocities of the emitted particles and the instants of their ejection (from the target surface) were calculated using the information from the subsequent camera frames (with visible traces of the particles flying from the target surface after a plasma shot) [11 - 20].

Pure tungsten of size 5×5×0.5 cm was used for the experiments. The combined W-C target consisting of a tungsten rod with a diameter of 1 cm surrounded by MPG-7 graphite with a diameter of 8 cm was also irradiated. The two types of CPS samples were exposed as well. The first sample included two stainless steel (SS) meshes wetted by Sn, placed in a copper target cap with a diameter of 5 cm. The average cell size of the mesh is 150×150 μm, the wire thickness is 90 μm [19]. The second CPS target was a cylindrical tungsten sample with a diameter of 2.45 cm and a height of 1.7 cm, filled with tin (the design is described in more detail in [8, 20]).

2. INVESTIGATION OF TRANSIENT PLASMA LAYERS DURING PLASMA SURFACE INTERACTION

Fig. 1 shows the heat load to the surfaces of tungsten, combined W-C, and tin (Sn) targets, measured using calorimetry, as a function of the energy density of the impacting plasma stream within QSPA Kh-50. Tungsten vapour shield formation and its influence on the plasma energy transfer to the surface become clearly seen as an impacting energy density achieves 2.4 MJ/m^2. The absorbed surface heat load does not exceed 1.1 MJ/m^2. The value of the heat load to the surface remains practically constant with further increase of the energy density of impacting plasma (see plateau region in Fig. 1). Plasma impacts with loads near the evaporation threshold cause the tungsten surface evaporation and the droplets splashing (Fig. 2,a).

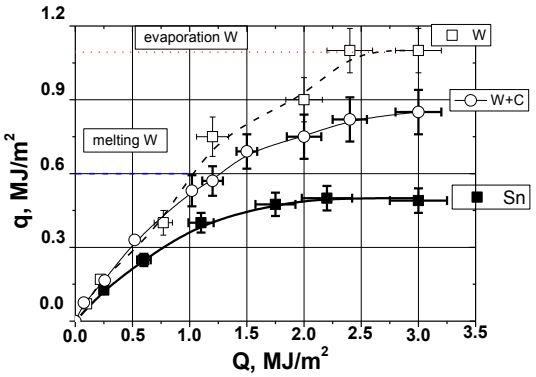

Fig. 1. Heat load to the target surfaces vs. the energy density of impacting plasma stream within QSPA Kh-50

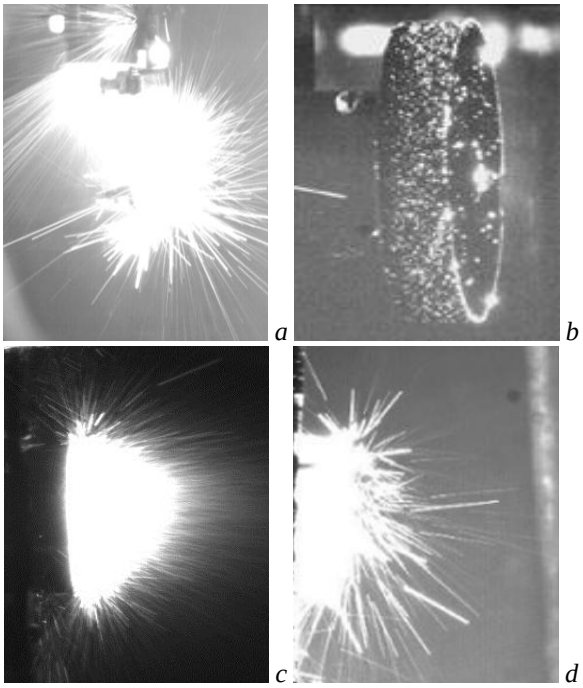

Fig. 2. Images of plasma stream interaction with different surfaces: W (a), W+C (b), Sn (c, d). The energy density of the exposing QSPA Kh-50 plasma stream is 2 MJ/m^2. Plasma impact is from right to left

Measurements of the energy transfer for the combined tungsten-graphite target demonstrate a reduction in the value of the energy density delivered to the target surface compared to tungsten irradiation alone. The formation of a carbon vapour shield during exposures of the combined W-C target results in an additional decrease in the heat loads to the W surface (from 1.1 to 0.8…0.85 MJ/m^2) and prevents tungsten evaporation. Hot spots are observed on the graphite surface of the combined W-C target (Fig. 2,b), indicating overheated local areas. The hot spots are likely formed due to the development of the relief on the graphite surface.

Evaporated tungsten is concentrated in a rather thin plasma layer of < 0.5 cm close to the surface and it does not propagate significantly upstream during the QSPA Kh-50 pulse. In the case of the graphite exhaust, the thickness of the shielding layer increases during the pulse and exceeds 5 cm. Spectroscopy measurements demonstrate that carbon lines are registered both in front of the target surface and at larger distances (at least up to 20 cm) from the target [10].

The shielding near the Sn surface develops at a lower impacting energy density (~ 1 MJ/m^2). The value of heat load to the CPS target is no more than 0.45 MJ/m^2. The energy density delivered to the CPS tin target is reduced compared to similar measurements performed for tungsten and W+C surfaces under identical treatment conditions. This result shows that for the CPS target, the energy shielding starts earlier and the shielding coefficient increases considerably due to the lower boiling temperature of T_{bSn} = 2875 K compared to tungsten boiling ($T_{bW} \approx 5933$ K) and carbon sublimation ($T_{bC} \approx 4000$ K) temperatures [9]. Nevertheless, particle emission is observed from the SS meshes wetted by Sn (Fig. 2,c) and from the CPS tungsten sample filled with Sn (Fig. 2,d). More intensive particle ejection is observed for the CPS tungsten target due to liquid particles leaving not only the Sn pool but also solid tungsten dust from the exposed matrix [20].

The influence of the magnetic field on the energy transfer to the exposed surface has been studied within QSPA-M. The maximum energy density of the free plasma stream achieved a value of Q = 0.75 MJ/m^2. No substantial difference has been observed in the energy density values of free plasma stream or their behaviour with and without a magnetic field [17 - 19].

High-speed images of plasma-surface interaction with tungsten and tin are presented in Fig. 3. The bright area in the images corresponds to the maximum density of the transient plasma layer that arises near the surface during the impact of the plasma stream. Moderated particle splashing is observed in the case of irradiation of tin target with plasma streams having an energy density of 0.75 MJ/m^2 within QSPA-M (see Fig. 3,b).

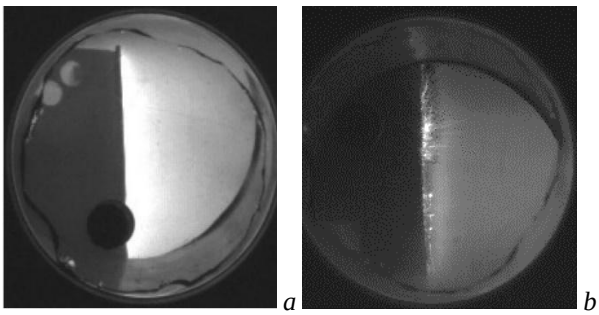

a *b*

Fig. 3. Images of plasma stream interaction with different surfaces: W (a), Sn (b). The energy density of the exposing QSPA-M plasma stream is 0.75 MJ/m^2. Plasma impact is from right to left

The heat load absorbed by the tungsten surface is approximately 60% of the impact plasma energy (Fig. 4). Nevertheless, such heat load caused the melting onset of the exposed tungsten surfaces. The heat load to Sn surfaces reached a saturation point at 0.3 MJ/m^2 under the same impacting energy conditions. The energy density in the shielding layer increases with the distance from the target surface. It illustrates the influence of the shielding effect during the plasma stream interaction with exposed surfaces (see Fig. 4). The energy density absorbed by the tin surface is lower compared to tungsten surfaces, as previously shown for QSPA Kh-50 (see Fig. 1).

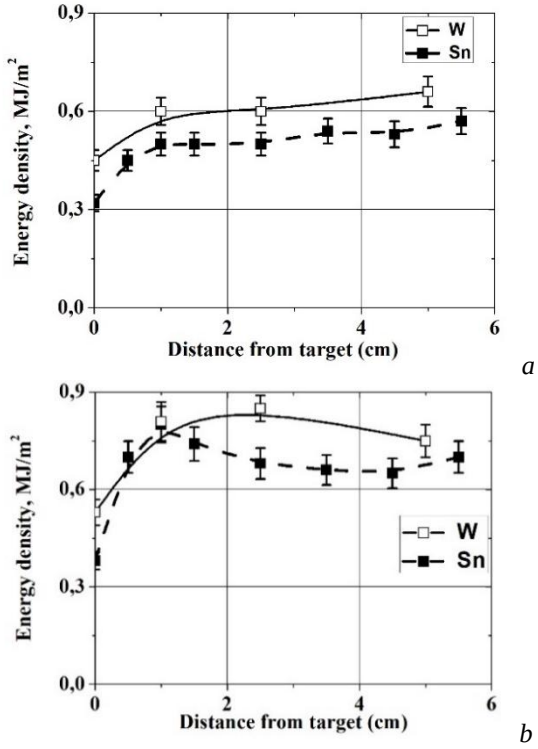

Fig. 4. Distributions of plasma energy density in the shielding layer vs the distance from the tungsten (W) and tin (Sn) target surfaces at different values of magnetic field (B) in QSPA-M: B = 0.8 T (a), B=0 (b). The energy density of the exposing QSPA-M plasma stream is 0.75 MJ/m^2

In the presence of an external magnetic field, the energy density saturates at a certain distance from the surface of both tin and tungsten samples. Only a part of the plasma energy is transferred to the target's surfaces through the shielding plasma layer (see Fig. 4,a). A different dynamics of energy dissipation in the shielding layer is observed without an external magnetic field. The energy density initially increases up to a maximum value within a layer of (1...2) cm, slightly exceeding the energy of the incident plasma. Afterward, the specific energy decreases with increasing distance and becomes comparable to the energy of the incident plasma. This behaviour is similar for both tungsten and tin surfaces (see Fig. 4,b). It could be attributed to the pinching effect and the formation of a current vortex near the exposed surface due to the compression of the head part of the plasma stream at the point of impact to the surface [10, 11].

Spectroscopy studies of plasma stream dynamics with and without an external magnetic field were also carried out. The measured chord-averaged plasma density in the shielding layer near the surface achieves a value in the range of $(2\ldots7)\cdot10^{23}$ m^{-3} [12, 13, 17, 19]. This value weakly depends on a further increase of the energy density in the plasma stream for both tin and tungsten targets. The electron density in the plasma shielding layer is found to be 5-10 times higher than in the impacting plasma stream. This dense plasma shield is completely non-transparent for the impacting plasma, being considerably larger in size than the particle free path length. It leads to a strong screening effect that

significantly reduces the plasma energy transfer to the surface [17 - 19].

The thickness of the shielding layer increases with the growth of the magnetic field. For small energy loads, the transient layer in front of the surface consists of plasma stream species only.

Sn lines are detected at distances of up to 3 cm from the exposed surface in the magnetic field of 0.8 T. The spectral lines of Sn were registered only in a very thin plasma layer near the exposed surface (< 0.5 cm from the surface) when the magnetic field was switched off. Thus, a magnetic field promotes the plasma shield confinement in front of the surface [19].

The tungsten spectral lines WI and WII start to appear only after the heat load exceeds the melting threshold of the material. Further increase of the energy load results in the development of a strong vapour shield consisting of both plasma and material ions. The evaporated tungsten is concentrated in a relatively thin plasma layer (of < 0.5 cm) near the surface. It does not significantly extend to greater distances upstream during the plasma pulse. This could be explained by a greater atomic mass of tungsten in comparison with carbon and tin. Due to the impacting plasma stream pressure and the flow of plasma around the target, the motion of evaporated tungsten around the target is also observed [17].

Radiation intensity near all kinds of samples is up to ten times higher when an external magnetic field is present compared to the case when there is no magnetic field (B=0) [17 - 19]. It is important to note that in the presence of an external magnetic field, visible radiation from the transient plasma layer is registered even after the end of a plasma pulse, as the sequence of plasma confinement in the shield is altered by the applied magnetic field.

CONCLUSIONS

Plasma energy transfer to surfaces has been evaluated during QSPA plasma interaction with surfaces of reference plasma-facing materials. The energy density of the impacting plasma streams achieved 3 MJ/m^2. Plasma layers are created near exposed surfaces. The electron density of the shielding layer is up to 10 times higher than in the impacting plasma stream.

The heat load to the combined carbon-tungsten target was about 80 percent of the energy density absorbed by tungsten surfaces. Nevertheless, carbon spectral lines were registered at large distances (up to 20 cm) compared to both tin (up to 3 cm) and tungsten (< 0.5 cm) materials. The disadvantage of carbon is its high ability to absorb tritium.

The energy density delivered to the capillary porosity system wetted by tin is half as small as that of a tungsten surface. The lower evaporation threshold of Sn causes a large shielding effect. Thus, the combined tungsten-tin target can mitigate the influence of the plasma stream with larger energy compared to pure tungsten samples. Nevertheless, a large splashing of particles accompanied plasma-surface interaction with the target wetted by tin. Therefore, the evolution of CPS target stabilities requires further experimental investigation at large heat loads.

ACKNOWLEDGEMENTS

This work has been carried out within the framework of the EUROfusion Consortium, funded by the European Union via the Euratom Research and Training Programme (Grant Agreement № 101052200-EUROfusion). Views and opinions expressed are however those of the author(s) only and do not necessarily reflect those of the European Union or the European Commission. Neither the European Union nor the European Commission can be held responsible for them. Work performed under EUROfusion WP PWIE.

This work has been supported by National Academy Science of Ukraine within the projects 22X-02-04/2023, 59-08/06-2023.

This work was supported in part by Simons Foundation/SFARI (Grant Number 1030288).

This work was supported in part by the Ministry of Education and Science of Ukraine within the joint Ukraine-Austria research project (UA 10/2023).

We are grateful to the Armed Forces of Ukraine and all the defenders of Ukraine from Russian aggression, as well as the solidarity and support from many governments and individuals around the world, which makes our future work possible.

REFERENCES

1. M. Reinhard et al. Latest results of Eurofusion plasma-facing components research in the areas of power loading, material erosion and fuel retention // *Nuclear Fusion*. 2022, v. 62, p**.** 042013.
2. J.H. You et al. Limiters for DEMO wall protection: Initial design concepts and technology options // *Fusion Engineering and Design*. 2002, v. 174, p. 112988.
3. G. Federici et al. Assessment of erosion of the ITER divertor targets during type I ELMs // *Plasma Physics and Controlled Fusion*. 2003, v. 45, p. 1523.
4. M. Rieth et al. Behavior of tungsten under irradiation and plasma interaction // *Journal of Nuclear Materials.* 2019, v. 519, p. 334-368.
5. M. Wirtz et al. Influence of helium induced nanostructures on the thermal shock performance of tungsten // *Nuclear Materials and Energy*. 2016, v. 9, p. 177-180.
6. M. Wirtz et al. High pulse number thermal shock tests on tungsten with steady state particle background // *Physica Scripta*. 2017, v. T170, p. 014066.
7. S. Roccella et al. CPS Based liquid metal divertor target for EU-DEMO // *Journal of Fusion Energy*. 2020, v. 39, p. 462-468.
8. P. Rindt et al. Conceptual design of a liquid-metal divertor for the European DEMO // *Fusion Eng. Des*. 2021, v. 173, p. 112812.
9. I.E. Garkusha et al. The latest results from ELM-simulation experiments in plasma accelerators // *Physica Scripta.* 2009, v. T138, p. 014054.
10. V.I. Tereshin et al. Application of powerful quasi-steady-state plasma accelerators for simulation of ITER transient heat loads on divertor surfaces //

Plasma Physics Controlled Fusion. 2007, v. 49, p. A231-A239.
11. V.A. Makhlai. Dynamics of the plasma streams generated by QSPA Kh - 50, during transportation in an external magnetic field // *Problems of Atomic Science and Technology. Series "Plasma Electronics and New Methods of Acceleration".* 2010, № 4, p. 94-99.
12. I.E. Garkusha et al. Novel test-bed facility for PSI issues in fusion reactor conditions on the base of next generation QSPA plasma accelerator // *Nuclear Fusion.* 2017, v. 57, p. 116011.
13. M.S. Ladygina et al. Parameters of hydrogen plasma streams in QSPA-M and their dependence on external magnetic field // *Problems of Atomic Science and Technology. Series "Plasma Physics"*. 2021, № 1, p. 61-64.
14. V.A Makhlaj. Characterization of QSPA plasma streams in plasma-surface interaction experiments: Simulation of ITER disruption // *Problems of Atomic Science and Technology. Series "Plasma Physics"*. 2012, № 6, p. 126-128.
15. V.A. Makhlaj. Characterization of QSPA plasma streams in plasma – surface interaction experiments: Simulation of ITER ELMS // *Problems of Atomic Science and Technology. Series "Plasma Physics"*. 2013, № 1, p. 73-75.
16. V.A. Makhlaj et al. Exposures of EU W-CFC combined targets with QSPA Kh-50 plasma streams simulating ITER ELMs // *Problems of Atomic Science and Technology*. *Series "Plasma Physics"*. 2009, № 1, p. 58-60.
17. I.E. Garkusha et al. Influence of a magnetic field on plasma energy transfer to material surfaces in edge-localized mode simulation experiments with QSPA-M // *Nuclear Fusion*. 2019, v. 59, p. 086023.
18. V.A. Makhlai et al. The effect of a small helium addition on the plasma-surface interaction in QSPA. // *Problems of Atomic Science and Technology*. *Series "Plasma Physics".* 2023, № 1, p. 63-66.
19. I.E. Garkusha et al. Vapour shielding of liquid-metal CPS-based targets under ELM-like and disruption transient loading // *Nuclear Fusion*. 2021, v. 61, p. 116040.
20. S.S. Herashchenko et al. The CPS's pre-heating effect on the capability to withstand extreme plasma loads // *Fusion Engineering and Design*. 2023, v. 190, p. 113527.

Article received 02.08.2023

ВНЕСОК ПЕРЕХІДНИХ ШАРІВ У ПЕРЕДАЧУ ЕНЕРГІЇ ПЛАЗМИ РІЗНИМ ПОВЕРХНЯМ ПРИ ВЗАЄМОДІЇ ПЛАЗМИ КСПП З ПОВЕРХНЯМИ

В.О. Махлай, І.Є. Гаркуша, С.С. Геращенко, Ю.Є. Волкова, Ю.В. Петров, М.М. Аксьонов, М.В. Кулик, Д.В. Єлісєєв, П.Б. Шевчук, Т.М. Меренкова

Передача енергії матеріалам, що контактуватимуть з плазмою в термоядерному реакторі нового покоління, а також відведення енергії та частинок повинні бути детально вивчені для реалізації проекту термоядерного реактора. Проведено аналіз особливостей взаємодії плазми з поверхнями при опроміненні в КСПП матеріалів, що обрані в якості основних матеріалів, які контактуватимуть з плазмою. Параметри плазмових потоків імітували умови перехідних процесів у термоядерному реакторі. Обговорено також вплив зовнішнього магнітного поля на енергетичний баланс при взаємодії плазми з поверхнями.